Latitude-dependent vertical mixing and the tropical thermocline in a global OGCM

V. M. Canuto,[1] A. Howard,[2] Y. Cheng, and R. L. Miller[1]

NASA Goddard Institute for Space Studies, New York, New York, USA

Received 4 March 2004; accepted 12 July 2004; published 19 August 2004.

[1] In most ocean general circulation models (OGCM), mixing in the pycnocline is treated with a constant background diffusivity. This creates the following problem. To obtain the observed sharp equatorial thermocline, OGCMs must adopt a pycnocline diffusivity ten times smaller than observed at mid-latitudes. The conflict can only be resolved by switching to a *spatially variable* mixing. In this work we present the GISS mixing model supplemented by *Gregg et al.*'s [2003] finding that the rate of dissipation of internal gravity waves is latitude dependent. We use the new GISS model in a global OGCM and obtain an equatorial thermocline in both the Atlantic and Pacific oceans that is sharper than without the latitude dependence. The model results for the Pacific compare favorably with *Kessler*'s [1990] data. The meridional overturning in the Atlantic and the global poleward heat transport are nearly unchanged from the values obtained without latitude dependence. *INDEX TERMS:* 4231 Oceanography: General: Equatorial oceanography; 4544 Oceanography: Physical: Internal and inertial waves; 4568 Oceanography: Physical: Turbulence, diffusion, and mixing processes; 4522 Oceanography: Physical: El Niño; 4255 Oceanography: General: Numerical modeling. **Citation:** Canuto, V. M., A. Howard, Y. Cheng, and R. L. Miller (2004), Latitude-dependent vertical mixing and the tropical thermocline in a global OGCM, *Geophys. Res. Lett.*, *31*, L16305, doi:10.1029/2004GL019891.

1. The Problem

[2] A sharp thermocline is both observed [*Kessler*, 1990] and required to reproduce reasonable ENSO variability [*Cane*, 1992]. To obtain it, one may adopt a low pycnocline heat diffusivity K_h. However, if used globally (as in models that employ a constant diffusivity), the resulting meridional overturning is far too weak. Thus, the challenge is to harmonize two contrasting requirements: an *average pycnocline* $K_h \cong 0.1\ cm^2s^{-1}$ to obtain a robust meridional overturning (16–25 Sv) [*Ganachaud*, 2003] and an *equatorial pycnocline* K_h some 10 times smaller. In this paper, the GISS mixing model, supplemented by the latitude-dependent rate of dissipation of internal gravity waves [*Gregg et al.*, 2003], is shown to satisfy both requirements.

2. The GISS Mixing Model

[3] The GISS mixing scheme [*Canuto et al.*, 2001, 2002] (hereinafter referred to as C1 and C2, respectively) is based on the Reynolds Stress Model and treats temperature and salinity as independent fields, thus incorporating double-diffusion processes. In general, the equations are time dependent and non-local. The solution of the local, stationary model yields the following expressions for the momentum, heat and salinity fluxes:

$$\langle w'u' \rangle = -K_m U_{,z}, \quad \langle w'T' \rangle = -K_h T_{,z}, \quad \langle w's' \rangle = -K_s S_{,z} \quad (1a)$$

We have used the notation $a_{,z} \equiv \partial a/\partial z$, brackets indicate a time or ensemble average and a prime denotes a fluctuating field; U, T and S are the mean velocity, temperature and salinity fields while the K_α's are the momentum, heat and salt diffusivities whose form can be given in two representations:

$$K_{\alpha 1} = \Gamma_{\alpha 1}\Lambda^2\Sigma \qquad K_{\alpha 2} = \Gamma_{\alpha 2}\,\varepsilon N^{-2} \qquad \Gamma_\alpha = \Gamma_\alpha\left(Ri, R_\rho\right) \quad (1b)$$

where Λ is a mixing length, Σ is the mean shear, N is the Brunt-Vaisala frequency and the Γ_α are mixing coefficients; $Ri = N^2/\Sigma^2$ is the Richardson number and $R_\rho = \alpha S_{,z}/\beta T_{,z}$ is the density ratio:(α, β) are the thermal expansion and haline contraction coefficients. While most models assume a single $\Gamma = 0.2$, the GISS model computes all the Γ_α (see Figure 7 of C2). Physically, the first representation in equation (1b) is used when the mixing is due to shear while the second representation is used when the mixing is due to internal wave breaking. In general, $K_{\alpha 1}$ dominates in the mixed layer while $K_{\alpha 2}$ dominates in the pycnocline. Since the two mixings may overlap, the physical diffusivity is the sum of the two contributions so as to assure a smooth transition between the two processes:

$$K_\alpha = K_{\alpha 1} + K_{\alpha 2} \quad (1c)$$

The turbulence model provides the Γ's while an expression for εN^{-2} has been provided by several authors [*Polzin et al.*, 1995; *Polzin*, 1996; *Kunze and Sanford*, 1996; *Gregg et al.*, 1996; *Toole*, 1998], and we have adopted the Gregg-Henyey-Polzin parameterization:

$$\varepsilon N^{-2} = 0.288\ cm^2s^{-1} \quad (1d)$$

Even though equation (1d) is a constant, $K_{\alpha 2}$ is not constant since $\Gamma_{\alpha 2}$ depends on Ri and R_ρ. The GISS mixing model was tested in: 1) 1D ocean models [*Burchard and Bolding*, 2001], 2) a 3D-OGCM vs. measured heat, salt and

[1]Also at Department of Applied Physics and Mathematics, Columbia University, New York, New York, USA.

[2]Also at Department of Earth, Atmospheric, and Planetary Sciences, Massachusetts Institute of Technology, Cambridge, Massachusetts, USA.

0094-8276/04/2004GL019891$05.00

concentration diffusivities (C2); 3) deep convection in the Labrador Sea [*Canuto et al.*, 2004] (hereinafter referred to as C4); 4) inter-comparison with other mixing models in non-convective regimes [*Halliwell*, 2004], 5) comparison with shear flow data (L. Umlauf, Modeling the effects of horizontal and vertical shear in stratified turbulent flows, submitted to *Deep Sea Research*, 2004).

3. Latitude-Dependent Diffusivities

[4] *Gregg et al.* [2003] reported measurements of a latitude-dependent $\varepsilon(\theta)$ which changes $K_{\alpha 2}$ to:

$$K_{\alpha 2} = \Gamma_{\alpha 2}\ \varepsilon_{30}\ N^{-2} L(\theta, N) \tag{2a}$$

where ε_{30} is defined by *Gregg et al.* [2003, equation (4)], while L is given by:

$$L(\theta, N) = [f\ \mathrm{Arccosh}(N/f)][f(30^\circ)\mathrm{Arccosh}(N_0/f(30^\circ)]^{-1} \tag{2b}$$

With the latitude dependence accounted for, $K_{\alpha 2}$ is now a function of Ri, R_ρ, N and f.

4. Global Tests

[5] We used the 3D NCAR-CSM ocean model with $3^\circ \times 3^\circ$ horizontal resolution, 25 vertical levels (7 levels in the upper 200 m) and a maximum depth of 5 km. We used the GM [*Gent and McWilliams*, 1990] parameterization for mesoscales with eddy advection and isopycnal diffusion coefficients equal to $8 \bullet 10^2 m^2 s^{-1}$. The OGCM was integrated to equilibrium for 126 years using split tracer and momentum time steps, with tracer time step ten times momentum throughout (see C1 and C4). Since Gregg et al. found diffusivities larger than the molecular value at the equator, we imposed a minimum of 0.07 on L in equation (2b). The global annually averaged temperature and salinity profiles with latitude dependence show little change compared to Figures 5–6 of C4 with no latitude dependence. The meridional overturning and poleward heat transport are hardly affected; the Atlantic meridional stream function is 1% larger than without latitude-dependent mixing and the northward heat transport for the entire ocean is reduced from 1.36 Pw to 1.25 Pw which are within the range of uncertainties of the data [*Macdonald and Wunsch*, 1996].

5. Tropical Atlantic

[6] In Figure 1 we show the Atlantic thermocline at 27°W, a location in the middle of the Atlantic away from land masses. We found similar results at 20°W close to Africa. Figure 1 shows model results together with Levitus data [*Antonov et al.*, 1998]. A sharpening of the thermocline in the middle panel is visible. To illustrate the difference, we computed the degree of stratification due to temperature, $N_h^2 = N^2(1 - R_\rho)^{-1}$. At the Equator and 27°W, at 62.5 m, the GISS model (no latitude dependence) yields $N_h^2 = 2.4\ 10^{-4}\ s^{-2}$ and $N_h^2 = 2.8\ 10^{-4}\ s^{-2}$ (with latitude dependence), indicating a sharpening. At 20°W, the corresponding values are $N_h^2 = 2.2\ 10^{-4}\ s^{-2}$ and $2.6\ 10^{-4}\ s^{-2}$, showing the same trend.

[7] In Figure 2, we show the annually averaged heat diffusivity in the Atlantic thermocline at 27°W from 45°S – to-45°N. Diffusivity varies widely with both latitude and depth. Values larger than 30 $cm^2 s^{-1}$ are due to weakly unstable gradients $N^2 \sim -10^{-6}\ s^{-2}$ and not internal wave breaking. Similar instabilities occur in the case without latitude dependence. The instabilities and the large associated diffusivities are not present at all times but persist for several days at a time and recur frequently so they contribute to the annual average. Diffusivities $>10^2\ cm^2\ s^{-1}$ are typical of the mixed layer [*Caldwell et al.*, 1997]. A z-variation of measured diffusivities [*Peters et al.*, 1988] shows a range almost as large as the one presented here.

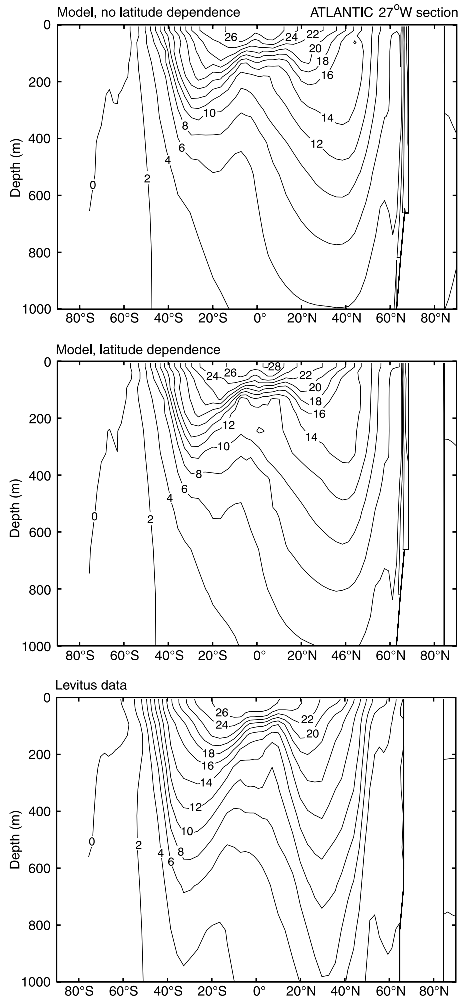

Figure 1. Annually averaged temperature sections at 27°W in the Atlantic with and without the latitude dependence. The two upper panels correspond to the GISS mixing model without and with latitude dependence while the lowest panel shows the Levitus data [*Antonov et al.*, 1998].

6. Tropical Pacific

[8] In most mixing models $K_{\alpha 1}$ is assumed to be a function of only the Richardson number Ri while $K_{\alpha 2}$ is taken to be a constant *background diffusivity*:

$$K_{\alpha 1} = f_\alpha(\mathrm{Ri}) \qquad K_{\alpha 2} = \mathrm{constant} \tag{3a}$$

The values of $K_{\alpha 2}$ for momentum and heat are K_{m2} = 1, K_{h2} = 0.1 [*Pacanowski and Philander*, 1981] (PP); K_{m2} =

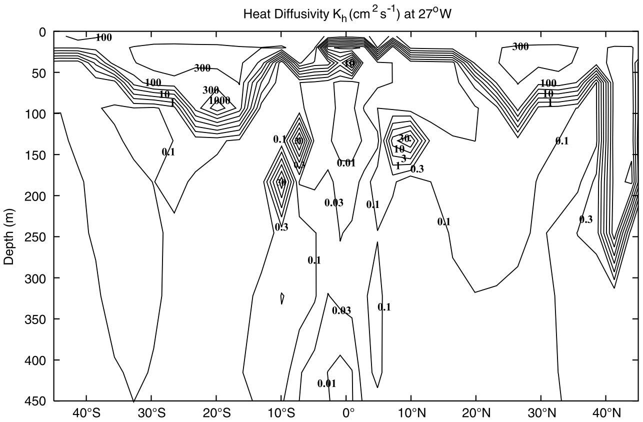

Figure 2. Annually averaged, latitude dependent heat diffusivity K_h (cm^{2}s^{-1}) at 27°W in the Atlantic.

0.2, K_{h2} = 0.01 [*Peters et al.*, 1988] (PGT); K_{m2} = 1 − 2, K_{h2} = 0.5 − 1 [*Gent*, 1991]; K_{m2} = 0.01, K_{h2} = 0 [*Latif et al.*, 1994; *Frey et al.*, 1997] (MPI); K_{m2} = 1, K_{h2} = 0.1 [*Chen et al.*, 1994] (Hybrid Vertical Mixing (HVM)); K_{m2} = 1, K_{h2} = 0.1 [*Large and Gent*, 1999] (KPP); K_{m2} = 2, K_{h2} = 0.2 [*Yu and Schopf*, 1997]; and K_{m2} = 0.2, K_{h2} = 0.01 [*Wilson*, 2000, 2002] (Integrated Power PGT model (IP)). The functions f_α(Ri) can be found in the references cited.

[9] *Wilson* [2000, 2002] analyzed four of the eight schemes, namely PP, PGT, MPI and IP and concluded that: 1) only PP is unable to yield a sharp thermocline and 2) that a much reduced set of values K_{m2} = 0.0134, K_{h2} = 0.1 K_{m2} (called the MPP, modified PP scheme) is needed to yield a sharp thermocline. The KPP model was tested by *Large and Gent* [1999] at four locations 165°E, 170°W, 140°W and 110°W. In the first two locations, the model reproduced the temperature profiles from TOGA-TAO while in the last two (corresponding to ENSO regions), the predicted thermocline was too diffuse, a behavior that Large and Gent attributed not to the vertical mixing model but to the uncertainties in the wind stress and heat flux forcing. The YS model at 110°W also yields a diffuse thermocline not very different from that of KPP. In the HVM model, the authors test three diffusivity models: a) a constant 50 m mixed layer plus *Gent*'s [1991] Ri-dependent model, b) a bulk mixing scheme and c) their own HVM. At 110°W, the HVM yields a slightly sharper thermocline than the other two models but still not in full accordance with the data. In summary, the above "background" values fall in the interval:

$$0.01 \le K_{h2}\left(\mathrm{cm^2s^{-1}}\right) \le 1 \tag{3b}$$

The lower value can yield a sharp thermocline but it is larger than the smallest value of *Gregg et al.* [2003] and if used globally, it yields a very weak meridional overturning. In Figure 3 we compare the longitudinal and latitudinal sections of the equatorial Pacific thermocline temperatures from the GISS model with the measured data [*Kessler*, 1990]. Along the Equator (left panels) the sharpening of the thermocline between 15–20°C is small, while the meridional sections show a somewhat greater improvement over the no-latitude dependence case. To quantify this behavior, in the zonal section, the distance between the 15–20°C isotherms at 160 W is 69 m (no latitude dependence) but 65 m (latitude dependence). In the meridional section, the distance between the same isotherms at the equator is 83 m (no latitude dependence) and 68 m with latitude dependence. The bulging out of isotherms has been reduced in the latitude-dependent case.

7. Conclusions

[10] In most mixing models, the pycnocline diffusivity is treated as a globally uniform, background value. The vertical diffusivity required for realistic meridional overturning and poleward heat transport [*Bryan*, 1991] results in an unrealistically diffuse tropical thermocline that inhibits ENSO variability [*Lau et al.*, 1992; *Miller and Jiang*, 1996]. Because of the global influence of ENSO [*Yulaeva and*

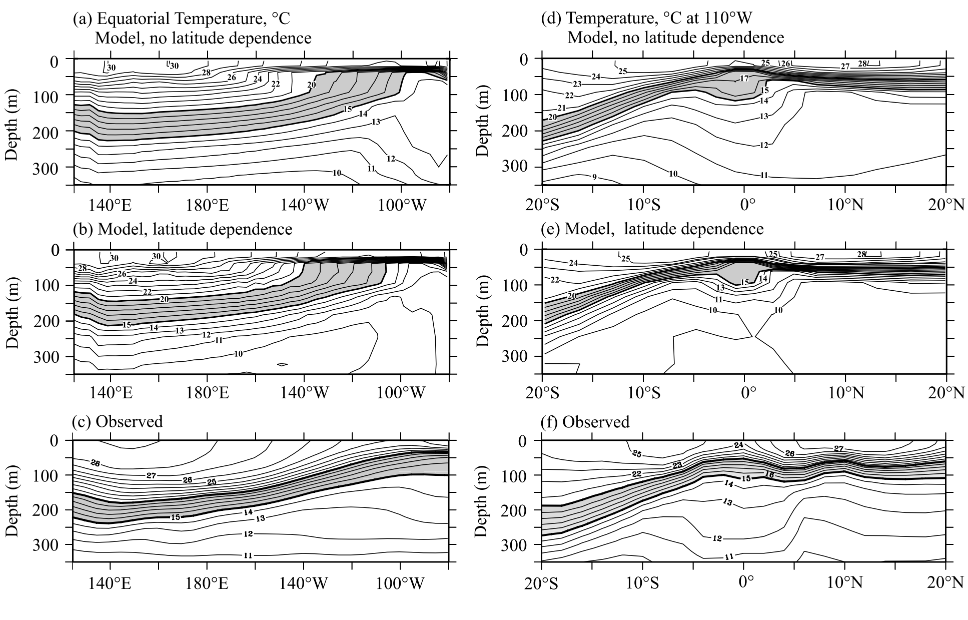

Figure 3. *Kessler* [1990] equatorial Pacific data vs. model predictions.

Wallace, 1994], this would distort the circulation of a coupled AGCM worldwide. The GISS model with latitudinal dependence of internal gravity wave dissipation [*Garrett*, 2003; *Gregg et al.*, 2003] yields both a robust North Atlantic stream function and a sharp thermocline. It may be of interest to notice that the latter was obtained using only 7 levels in the upper 200 m, a modest number compared to typical ENSO simulations with an OGCM [*Philander et al.*, 1992]. The present results are an attempt to account for a spatially variable turbulent kinetic energy dissipation rate ε in an OGCM. We have accounted for the latitude dependence in the pycnocline but an additional source of spatial variability represents tidal energy dissipation in the ocean's bottom [*Simmons et al.*, 2004]. Once the latter is added to the GISS model, we hope to obtain an even more complete representation of mixing from the surface to the ocean's bottom. Work in that direction is under way.

[11] **Acknowledgments.** The authors thank Dr. W. S. Kessler for providing the data of Figure 3 and Drs. S. G. Wilson, A. Romanou and G. Tselioudis for useful comments. The authors thank the NASA Climate Program and NASA Oceanography Program managed by Tsengdar Lee and Eric Lindstrom for financial support. A.Howard thanks the Physical Oceanography Division of NSF for partial financial support (NSF OCE –0241668).

References

Antonov, J., S. Levitus, T. P. Boyer, M. Conkright, T. O'Brien, and C. Stephens (1998), *World Ocean Atlas*, vol. 1, *Temperature of the Atlantic Ocean*, *NOAA Atlas NESDIS*, vol. 27, 166 pp., U. S. Gov. Print. Off., Washington, D. C.

Bryan, K. (1991), Poleward heat transport in the ocean, *Tellus*, *34*, 104–115.

Burchard, H., and K. Bolding (2001), Comparative analysis of four second order turbulence closure models for the ocean mixed layer, *J. Phys. Oceanogr.*, *31*, 1943–1968.

Caldwell, D. R., R. C. Lien, J. N. Moum, and M. C. Gregg (1997), Turbulence decay and stratification in the equatorial ocean surface layer following nighttime convection, *J. Phys. Oceanogr.*, *27*, 1120–1132.

Cane, M. A. (1992), Tropical Pacific ENSO models: ENSO as a mode of the coupled system, in *Climate System Modeling*, edited by K. E. Trenberth, pp. 583–614, Cambridge Univ. Press, New York.

Canuto, V. M., A. Howard, Y. Cheng, and M. S. Dubovikov (2001), Ocean turbulence, part I: One-point closure model momentum and heat vertical diffusivities, *J. Phys. Oceanogr.*, *32*, 1413–1426.

Canuto, V. M., A. Howard, Y. Cheng, and M. S. Dubovikov (2002), Ocean turbulence, part II: Vertical diffusivities of momentum, heat, salt, mass and passive scalars, *J. Phys. Oceanogr.*, *32*, 240–264.

Canuto, V. M., A. Howard, P. Hogan, Y. Cheng, M. S. Dubovikov, and L. M. Montenegro (2004), Modeling ocean deep convection, *Ocean Modell.*, *7*, 75–95.

Chen, D., L. M. Rothstein, and A. J. Busalacchi (1994), A hybrid vertical mixing scheme and its application to tropical ocean models, *J. Phys. Oceanogr.*, *24*, 2156–2179.

Frey, H., M. Latif, and T. Stockdale (1997), The coupled GCM ECHO-2. Part I: The tropical Pacific, *Mon. Weather Rev.*, *125*, 703–720.

Ganachaud, A. (2003), Large-scale mass transports, water mass formation and diffusivities from WOCE, *J. Geophys. Res.*, *108*(C7), 3213, doi:10.1029/2002JC001565.

Garrett, C. (2003), Mixing with latitude, *Nature*, *422*, 477–478.

Gent, P. R. (1991), The heat budget of the TOGA-COARE domain in an ocean model, *J. Geophys. Res.*, *96*, 3323–3330.

Gent, P. R., and J. C. McWilliams (1990), Isopycnal mixing in ocean circulation models, *J. Phys. Oceanogr.*, *20*, 150–155.

Gregg, M. C., D. P. Winkel, T. S. Sanford, and H. Peters (1996), Turbulence produced by internal waves in the ocean thermocline at mid and low latitudes, *Dyn. Atmos. Oceans*, *24*, 1–14.

Gregg, M. C., T. B. Sanford, and D. P. Winkel (2003), Reduced mixing from the breaking of internal waves in equatorial waters, *Nature*, *422*, 513–515.

Halliwell, G. (2004), Evaluation of vertical coordinate and vertical mixing algorithms in the Hybrid Coordinate Ocean Model (HYCOM), *Ocean Modell.*, *7*, 285–322.

Kessler, W. S. (1990), Observations of long Rossby waves in the northern tropical Pacific, *J. Geophys. Res.*, *95*, 5183–5217.

Kunze, E., and T. S. Sanford (1996), Abyssal mixing: Where it is not, *J. Phys. Oceanogr.*, *26*, 2286–2296.

Large, W. G., and P. R. Gent (1999), Validation of vertical mixing in an equatorial ocean model using LES and observations, *J. Phys. Oceanogr.*, *29*, 449–464.

Latif, M., T. Stockdale, J. Wolff, G. Burgers, E. Maier-Raimer, M. M. Junge, K. Arpe, and L. Bengston (1994), Climatology and variability in the ECHO coupled GCM, *Tellus*, *46*, 351–366.

Lau, N.-C., S. G. H. Philander, and M. J. Nath (1992), Simulation of ENSO-like phenomenon with a low resolution coupled GCM of the global atmosphere, *J. Clim.*, *5*, 284–307.

Macdonald, A. M., and C. Wunsch (1996), An estimate of global circulation and heat fluxes, *Nature*, *382*, 436–439.

Miller, R. L., and X. Jiang (1996), Surface energy fluxes and coupled variability in the tropics of a coupled general circulation model, *J. Clim.*, *9*, 1599–1620.

Pacanowski, R. C., and S. G. H. Philander (1981), Parameterization of vertical mixing in numerical models of tropical oceans, *J. Phys. Oceanogr.*, *11*, 1443–1451.

Peters, H., M. C. Gregg, and J. M. Toole (1988), On the parameterization of equatorial turbulence, *J. Geophys. Res.*, *93*, 1199–1218.

Philander, S. G. H., R. C. Pacanowski, N.-C. Lau, and M. J. Nath (1992), Simulation of ENSO with a global atmospheric AGCM coupled to a high resolution tropical Pacific Ocean GCM, *J. Clim.*, *5*, 308–329.

Polzin, K. (1996), Statistics of the Richardson number: Mixing models and fine structure, *J. Phys. Oceanogr.*, *26*, 1409–1425.

Polzin, K., J. M. Toole, and R. W. Schmitt (1995), Fine scale parameterization of turbulent dissipation, *J. Phys. Oceanogr.*, *25*, 306–328.

Simmons, H. L., S. R. Jayne, L. C. St. Laurent, and A. J. Weaver (2004), Tidally driven mixing in a numerical model of the ocean general circulation, *Ocean Modell.*, *6*, 245–263.

Toole, J. M. (1998), Turbulent mixing in the ocean, in *Ocean Modeling and Parameterization*, *NATO ASI Ser. C*, vol. 516, pp. 171–190, edited by E. P. Chassignet and J. Verron, Kluwer Acad., Norwell, Mass.

Wilson, S. G. (2000), How ocean vertical mixing and accumulation of warm surface water influences the "sharpness" of the equatorial thermocline, *J. Clim.*, *13*, 3638–3656.

Wilson, S. G. (2002), Evaluation of various vertical mixing parameterizations in a tropical Pacific Ocean GCM, *Ocean Modell.*, *4*, 291–311.

Yu, Z., and P. S. Schopf (1997), Vertical eddy mixing in the tropical upper ocean: Its influence on zonal currents, *J. Phys. Oceanogr.*, *27*, 1447–1458.

Yulaeva, E., and J. M. Wallace (1994), The signature of ENSO in global temperature and precipitation fields derived from the Microwave Sounding Unit, *J. Clim.*, *7*, 1719–1736.

V. M. Canuto, Y. Cheng, A. Howard, and R. L. Miller, NASA Goddard Institute for Space Studies, 2880 Broadway, New York, NY 10025, USA. (vcanuto@giss.nasa.gov)